

Synergistic Impact of Nicotine and Shear Stress Induces Cytoskeleton Collapse and Apoptosis in Endothelial Cells

YU-HSIANG LEE,¹ RUEI-SIANG CHEN,¹ NEN-CHUNG CHANG,² KUEIR-RARN LEE,³ CHIEN-TSAI HUANG,⁴
YU-CHING HUANG,⁵ and FENG-MING HO^{2,3,4}

¹Graduate Institute of Biomedical Engineering, National Central University, Taoyuan County, Taiwan, ROC; ²Department of Internal Medicine, School of Medicine, Taipei Medical University, Taipei, Taiwan, ROC; ³R&D Center for Membrane Technology, Department of Chemical Engineering, Chung Yuan Christian University, Taoyuan County, Taiwan, ROC; ⁴Department of Internal Medicine, Tao-Yuan General Hospital, Ministry of Health and Welfare, 1492 Chung Shan Rd., Taoyuan County 33004, Taiwan, ROC; and ⁵Department of Neurology, Tao-Yuan General Hospital, Ministry of Health and Welfare, Taoyuan County, Taiwan, ROC

(Received 20 September 2014; accepted 29 December 2014; published online 29 January 2015)

Associate Editor Sriram Neelamegham oversaw the review of this article.

Abstract—Nicotine is the major component in cigarette smoke and has been recognized as a risk factor for various cardiovascular diseases such as atherosclerosis. However, the definite pathogenesis of nicotine-mediated endothelial dysfunction remains unclear because hemodynamic factor in most of prior *in vitro* studies was excluded. To understand how nicotine affects endothelium in the dynamic environment, human umbilical vein endothelial cells were treated by different laminar shear stresses (LSS; 0, 6, 8, and 12 dynes cm⁻²) with and without 10⁻⁴ M nicotine for 12 h in a parallel plate flow system, following detections of cellular morphology and apoptotic level. Our results showed that cells sheared by 12 dynes cm⁻² LSS with nicotine excessively elongated and aligned with the flow direction, and exhibited significant apoptosis as compared to the groups with nicotine or LSS alone. We reasoned that the irregular morphological rearrangement and elevated apoptosis were resulted from the interruption of mechanostasis due to cytoskeletal collapse. Furthermore, all the impaired responses can be rescued by treatment with free radical scavenger ascorbic acid (10⁻⁴ M), indicating oxidative stress was likely mediated with the impairments. In summary, our findings demonstrated an essential role of LSS in nicotine-mediated endothelial injury occurring in the physiological environment.

Keywords—Nicotine, Laminar shear stress, Morphological reorganization, Cytoskeleton disintegration, Apoptosis.

INTRODUCTION

Among more than 4700 chemical constituents of cigarette smoke, nicotine is the major component and a leading risk factor for pathogenesis of atherosclerosis,¹⁷ a systemic and multifocal symptom that may develop to diverse cardiovascular diseases subsequently. Although the biological effects and functions of nicotine has been well investigated in the past decades,⁴ yet the definite mechanisms of nicotine-induced endothelial dysfunctions are not completely understood. That is mainly because most of prior *in vitro* studies precluded hemodynamic factors that play a critical role in modulating endothelial phenotypes and functions.²

Knowingly vascular endothelial cells *in vivo* are influenced by two distinct hemodynamic forces: cyclic strain due to vessel wall distention by transmural pressure, and laminar shear stress (LSS), the frictional force generated by blood flow. Endothelial cells normally respond to LSS by releasing vasoactive substances³³ and altering morphology by which cells elongate and align with the flow direction.¹⁸ This cytoskeletal reorientation triggers a variety of intracellular signaling cascades and influences formation of stress fibers and focal adhesions that collectively confer endothelial protection such as anti-inflammation³⁰ and anti-atherosclerosis.²⁸ In otherwise healthy individuals, atherosclerotic lesions generally occur at bifurcations and sharp curves where the blood flow is interrupted and the mean LSS is low (<4 dynes cm⁻²).^{21,29} However, a plethora of clinical studies have shown that smoking-mediated atherosclerotic development does not follow this pattern. Instead,

Address correspondence to Feng-Ming Ho, Department of Internal Medicine, Tao-Yuan General Hospital, Ministry of Health and Welfare, 1492 Chung Shan Rd., Taoyuan County 33004, Taiwan, ROC. Electronic mail: heart@mail.tygh.gov.tw

there is a strong association between smoking and large (proximal) vessel (e.g., aorta artery) disease¹ where the LSS is certainly higher than 4 dynes cm⁻².³⁴ In addition, it has been recognized that smoking is a major and modifiable risk factor for peripheral arterial disease (PAD), and all of the related studies consistently showed that the smoking-related PAD affects predominantly proximal arteries, especially the aorta and iliac arteries.^{9,25} Haltmayer *et al.*¹³ have further reported the odds ratio gradient of PAD in the presence of smoking, indicating that the smoking-mediated PAD is in a strong association with aortoiliac lesion; a lower but still significant association at the femoropopliteal level, and no association at the crural level. This substantial correlation leads to our hypothesis that high shear stress may play a role in vascular injury while endothelial cells are exposed to nicotine.

Apoptosis is a regulated process for disposal of unwanted cells and is necessary for maintaining homeostasis. Currently there is ongoing debate that whether nicotine functions as an inducer or inhibitor of endothelial apoptosis under static culture. Although most studies point towards a more anti-apoptotic effect, some efforts presented an opposite result (i.e., pro-apoptotic effect).³⁵ This conflict is probably resulted from diverse models used for the investigations, different analytic approaches, and/or subjective interpretations of the data. In terms of the correlation between LSS and endothelial apoptosis, most studies coherently exhibited that shear stress can inhibit cellular apoptosis induced by external stimuli such as toxicants, cytokines, and extracellular microenvironment change through modulations of intracellular nitric oxide,¹⁰ gene expression,²⁴ and/or stress fibers reorganization.³¹ However, to the best of our knowledge, very little information is referred to the apoptosis of endothelial cells treated by nicotine and LSS simultaneously.

In this paper, we attempt to study how endothelial cells are affected by association of nicotine and LSS using an *in vitro* laminar shearing device to mimic the hemodynamic environment in vasculature. The synergistic effects of nicotine and LSS on the cell morphological alteration and expression of apoptosis were first examined, and the role of LSS in nicotine-mediated endothelial impairments was then investigated. Furthermore, the potential mechanism of the cellular impairments led by incorporation of nicotine and LSS was reported.

MATERIALS AND METHODS

Cell Culture and Reagents

Human umbilical vein endothelial cells (HUVECs; Lonza, Walkersville, MD) were cultured using Medium 199 supplemented with 20% fetal bovine serum

(Biological Industries, Kibbutz Beit Haemek, Israel), endothelial cell growth supplement (Millipore, Billerica, MA), 0.1% heparin sodium, 1% L-glutamine, and 1% penicillin/streptomycin (Biological Industries) in tissue culture flasks at 37 °C with 5% CO₂. HUVECs at passage of 3–5 were transferred to sterilized gelatin-coated glass slides with 1.5×10^6 cells for each, and incubated for 24 h prior to the experiments. Both nicotine ((-)-nicotine, Sigma, St. Louis, MO) and ascorbic acid (Sigma) were used at concentration of 10^{-4} M in the experiments. All reagents were used as received.

LSS Setup

To apply LSS on the cell surface, each glass slide (76 mm × 38 mm × 1.0 mm) seeded with HUVECs was placed in the parallel plate flow chamber which was connected to a laminar flow system as illustrated in Supplementary Fig. S1. The magnitude of LSS (τ) on the cell monolayer was calculated using Navier–Stokes equation for Newtonian fluid in the parallel plate geometry:

$$\tau = \frac{6\mu Q}{bh^2} \quad (1)$$

where μ is the viscosity of the media (0.01 dynes s cm⁻²), Q is the volumetric flow rate, b is the width of the flow chamber, and h is the distance between the chamber and the glass slide as indicated in Supplementary Fig. S1. In this study, the flow media used in all of the shearing experiments were the cell culture medium which was described above. In addition, intensities of 0, 6, 8, and 12 dynes cm⁻² were used to simulate different levels of LSS in vasculature that the average physiological LSS is approximately 6–10 dynes cm⁻².^{21,12} in which the low LSS may occur in venous system with intensity of 1–6 dynes cm⁻²²²¹ while the high LSS of 10–16 dynes cm⁻² is usually presented in the proximal arteries (e.g., aorta and iliac vessels).³⁴ In this study, the maximal magnitude of 12 dynes cm⁻² was employed to simulate the LSS in the aorta.³⁴ Each LSS can be obtained by setting appropriate flow rate according to the Eq. (1). Cells used for the shearing experiments will be treated by nicotine, LSS, and/or ascorbic acid simultaneously.

Imaging Analysis for Morphological Reorganization

To quantitatively evaluate how nicotine or combination of nicotine and ascorbic acid affects cellular response to LSS, the aspect ratio (AR; major/minor axis of a cell) and the angle between cellular major axis and the flow direction (AMAF) of each cell were measured. For each slide, six areas away from the edge were photographed using an inverted microscope before and after

LSS treatment, following measurements of AR and AMAF of each cell using NIS-Elements BR 3.0 software (Nikon, Melville, NY). Results from the six images containing ≥ 1500 cells were pooled and each cell was counted as a single data point for subsequent analyses. To avoid results misjudgment caused by originally different cell phenotype between slides, cell responses to LSS in each group were presented by variations of AR (Δ AR) and AMAF (Δ AMAF) obtained from normalization to the value acquired before LSS treatment.

Immunostaining and Western Blot

The stress fibers (i.e., actin cytoskeletons) and cell nuclei were stained by using rhodamine phalloidin (Sigma, 1:200) and Hoechst 33258 (Sigma, 1:1000), respectively according to the previous report,³¹ and photographed through fluorescence microscopy. Protein expressions of actin (Pan-actin, Cell signaling, Danvers, MA), α -tubulin (Cell signaling), Poly(ADP-ribose) polymerase 1 (PARP1; Cell signaling) and glyceraldehyde 3-phosphate dehydrogenase (GAPDH; Cell signaling) were detected using Western blot as reported in elsewhere.²³ GAPDH was used as the reference protein in this study.

Apoptosis Assay

Cellular apoptosis was quantitatively measured by DNA fragmentation assay using Cell Death Detection ELISA^{PLUS} Kit (Roche, Indianapolis, IN) according to the manufacturer's instruction. The absorbance of anti-DNA-peroxidase (POD) molecules associated with cytoplasmic histone-associated DNA fragments induced from the apoptotic cells was detected using the fluorescent microplate reader (GENios Plus; TECAN, Maennedorf, Switzerland) set at 405 nm wavelength. The absorbance values were analyzed after normalization to the background signal.

Statistics

All data were obtained from triplicate experiments and presented as mean \pm standard error (SE). Statistical analyses were conducted using MedCalc software in which comparisons for one condition between two sample sets were performed at a significance level of $p < 0.05$ based on Student's *t* test followed by Dunnett's *post hoc* test throughout the study.

RESULTS

Nicotine Enhanced Morphological Reorganization Induced by LSS

Figure 1 showed morphological changes of HUVECs sheared with 0 (static culture), 6, 8, and 12 dynes cm^{-2}

LSS for 12 h using normal and nicotine media (10^{-4} M), respectively. We found cells shrank in static cultivation with nicotine (Fig. 1b; mean AR = 3.87 ± 0.43) that the AR significantly increased about 60% ($p < 0.05$) as compared to the group without nicotine exposure (Fig. 1a; mean AR = 2.41 ± 0.36), and both cells grew in arbitrary arrangement without preferred orientation. For the shearing cultures, cells in all settings elongated and aligned with the flow direction as reported in the previous studies,¹⁸ and the level of morphological reorganization enhanced along with the increase of LSS intensity used. This alteration was more pronounced in the nicotine-treated groups that cells significantly converted from typical spindle-like shape (Fig. 1f) to slim strip (Fig. 1h) when the LSS was elevated from 6 to 12 dynes cm^{-2} . In terms of the result of morphological measurement, both Δ AR (Fig. 2a) and Δ AMAF (Fig. 2b) augmented with increase of LSS intensity regardless of using normal or nicotine medium, and exhibited significant increase of 72 and 46% ($p < 0.05$), respectively in the nicotine-treated group sheared by 12 dynes cm^{-2} LSS. Furthermore, the synergistic effect of 12 dynes cm^{-2} LSS and low concentration of nicotine (10^{-7} M) on HUVECs was additionally examined as shown in Supplementary Fig. S2. Our results showed that the morphologies of sheared cells with (Fig. S2(B)) and without (Fig. S2(A)) nicotine were similar within 12 h of shearing. Nicotine-treated cells exhibited excessive morphological reorganization while the shearing time was extended to 24 h (Fig. S2(C) vs. (D)). These results manifested that nicotine may enhance the morphological reorganization of endothelial cells induced by LSS.

Synergistic Effect of Nicotine and LSS Enhanced Apoptotic Level of HUVECs

To assess the effect of excessive morphological change on cell fate, the apoptosis of HUVECs treated with different intensities of LSS in the presence and absence of 10^{-4} M nicotine was examined. Figure 3a exhibited photomicrographic images of Hoechst staining HUVECs under various treatments in which intense blue stains represented apoptotic DNA fragments in the nuclei. Our result showed that the percentage of apoptotic cells in the control group (Fig. 3a(A)) was about 3.8% which is similar to the data reported previously,¹⁹ manifesting that the cellular apoptosis was not affected by the glass slide-mediated cultivation. Furthermore, it can be observed that neither nicotine (Fig. 3a(E)) nor LSS treatment (Fig. 3a(B, C, D)) alone enabled to cause marked apoptotic features as compared to the static culture without nicotine (Fig. 3a(A)). However, the cellular apoptosis dramatically raised along with increase of LSS intensity used in the presence of 10^{-4} M nicotine

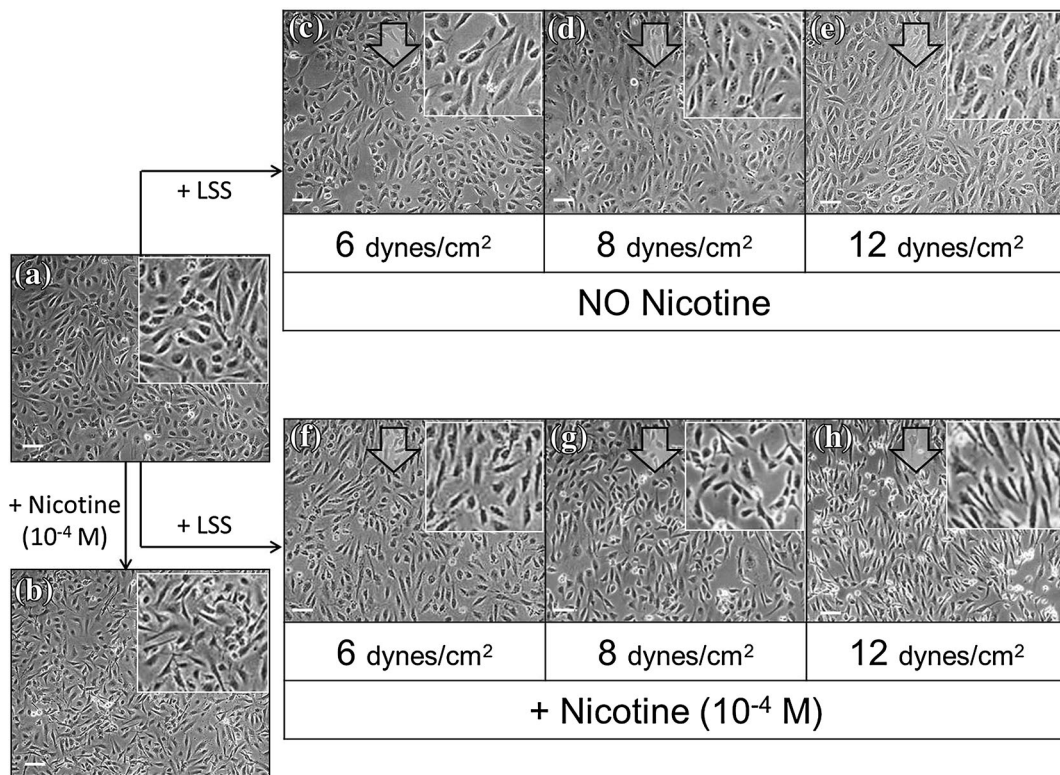


FIGURE 1. Photomicrographic images of HUVECs under various treatments of nicotine and LSS. (a) Cells were statically cultured using normal medium; (b) cells were statically cultured with 10^{-4} M nicotine for 12 h. Cells were sheared by 6 (c, f), 8 (d, g), and 12 (e, h) dynes cm^{-2} using normal (c, d, e) and/or nicotine-containing medium (f, g, h) for 12 h. Images were photographed at $20\times$ magnification. Arrows indicate the flow direction. Scale bar = $100\ \mu\text{m}$.

(Fig. 3a(E–H)). Through the detection of the absorbance of cytoplasmic histone-associated DNA fragments (Fig. 3b), we found that the apoptosis of cells up- and down-regulated with the LSS intensity used in the presence and absence of nicotine, respectively, by which the cellular apoptosis significantly increased 40% (+ nicotine) and decreased 43% (– nicotine; $p < 0.05$ for both) when the LSS was elevated from 0 to 12 dynes cm^{-2} . Furthermore, cells with nicotine exhibited a 1.3-, 1.4-, 2-, and 3-fold ($p < 0.05$) higher apoptotic level than the cultures without nicotine exposure under 0, 6, 8, and 12 dynes cm^{-2} LSS treatment, respectively. Similar results can be found in the studies where 10^{-7} M nicotine was utilized as shown in Supplementary Fig. S3. Our data showed that the apoptotic level of cells treated with 10^{-7} M nicotine and 12 dynes cm^{-2} LSS for 24 h significantly increased 50.4% ($p < 0.05$) as compared to the nicotine-treated cells (10^{-7} M) without shearing, and was 2.6-fold ($p < 0.05$) higher than the LSS-treated group without nicotine. The synergistic effect of 10^{-4} M nicotine and 12 dynes cm^{-2} LSS on endothelial apoptosis was further examined by detection of PARP1 expression as shown in Fig. 4. Our data showed that the intensity ratio of fragment to full length of PARP1 in the cells with both stimulations (Fig. 4; LSS + N) remarkably

increased 13- and 5-fold as compared to the group treated with LSS alone (Fig. 4; LSS + N vs. LSS) and nicotine alone (Fig. 4; LSS + N vs. N), respectively. These data exhibited that high LSS may further induce endothelial death in the presence of nicotine.

Synergistic Impact of Nicotine and LSS Induced Cytoskeletal Disintegration of HUVECs

Figure 5 exhibited photomicrographic images of immunostained HUVECs under nicotine and/or LSS treatment for 12 h. It can be observed that 10^{-4} M nicotine caused slight depletion of cytoskeletal filaments near the nuclei (Fig. 5c) while the 12 dynes cm^{-2} LSS alone can barely reorient the cytoskeletal filaments into a parallel arrangement without detrimental effect (Fig. 5b). However, synergistic impact of nicotine and LSS may severely damage the cytoskeleton since a lot of filaments collapsed particularly near the nuclei (Fig. 5d).

The expressions of cytoskeletal molecules of actin and α -tubulin were further examined as shown in Fig. 6. Our results showed that both molecules down-regulated in the group with nicotine and LSS stimulations that the expression of actin significantly decreased 48 and 52%, whereas α -tubulin decreased 44

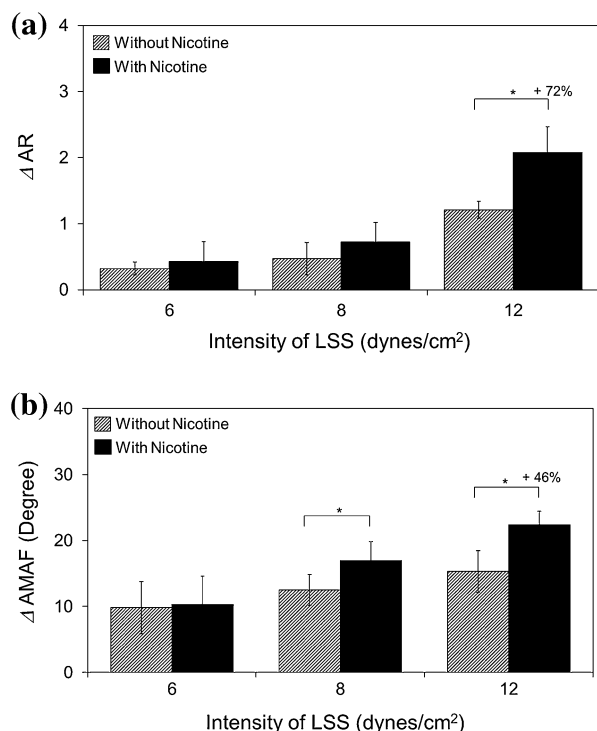


FIGURE 2. Effect of synergistic effect of nicotine and LSS on the morphological reorganization of HUVECs. The cellular elongation (a) and reorientation (b) after sheared by 6, 8, and 12 dynes cm^{-2} LSS in the presence and absence of 10^{-4} M nicotine were quantitatively analyzed by calculating the ΔAR and ΔAMAF , respectively. ΔAR = the mean AR after LSS treatment—the mean AR before LSS treatment. ΔAMAF = the mean AMAF before LSS treatment—the mean AMAF after LSS treatment. Values are mean \pm SE ($n = 3$). * $p < 0.05$.

and 41% as compared to the group with LSS (Fig. 6; LSS vs. LSS + N) or nicotine (Fig. 6; N vs. LSS + N) alone, respectively ($p < 0.05$ for all comparisons). These results demonstrated that synergistic impact of 12 dynes cm^{-2} LSS and 10^{-4} M nicotine can certainly damage the cytoskeletal filaments of HUVECs within 12-h treatment.

Ascorbic Acid Mitigated Irregular Morphological and Cytoskeletal Rearrangement

Figure 7 exhibited the efficacy of using ascorbic acid, a common free radical scavenger to reduce the excessive morphological reorganization and cytoskeletal collapse caused by synergistic impact of nicotine and LSS. It can be observed that 10^{-4} M ascorbic acid was able to reduce the magnitudes of cell elongation and alignment (Fig. 7a), where the ΔAR and ΔAMAF of ascorbic acid-treated cells significantly decreased 35 and 30% ($p < 0.05$ for each), respectively as compared to the nicotine and LSS-treated group without ascorbic acid, and exhibited similar level to the control ($p = \text{NS}$ for both). Moreover, the cytoskeletal disintegration of

the cells with 10^{-4} M ascorbic acid was mitigated (Fig. 7b), by which the expressions of actin and α -tubulin (Fig. 7b; LSS + N + A) significantly increased 36 and 32% ($p < 0.05$ for each), respectively as compared to the setting without ascorbic acid (Fig. 7b; LSS + N). These results exhibited that the impaired morphological reorganization and cytoskeletal filaments of HUVECs led by nicotine and LSS can be rescued by use of ascorbic acid.

Ascorbic Acid Reduced Apoptosis of HUVECs Induced by Nicotine and LSS

The effect of ascorbic acid on the concomitant apoptosis was subsequently examined using DNA fragmentation assay and detection of PARP1 expression as presented in Fig. 8. Our data showed that the absorbance of ascorbic acid-treated cells (Fig. 8; LSS + N + A) significantly reduced 2.5 fold ($p < 0.05$) as compared to the group without ascorbic acid (Fig. 8; LSS + N), and was similar to the control (Fig. 8; LSS; $p = \text{NS}$). In addition, the intensity ratio of fragment to full length of PARP1 in the group with ascorbic acid (Fig. 8; LSS + N + A) significantly diminished about 2 fold ($p < 0.05$) as compared to the same setting without ascorbic acid (Fig. 8; LSS + N). These outcomes showed that the apoptosis induced by the synergistic impact of nicotine and LSS can be greatly reduced by use of ascorbic acid.

DISCUSSION

Both nicotine and LSS have been recognized as important factors for atherosclerosis. Despite conflicting results can be found in each vascular territory, there is a suggestion of a strong association between smoking and large vessel disease based on a plethora of clinical studies,^{1,13,26} implicating that the hemodynamic factor may play a role in nicotine-mediated vascular diseases. However, endothelial-related study involving both nicotine and LSS is scarce, leading to the definite pathogenesis of nicotine-mediated endothelial injury remains unclear. In this study we aimed to study how endothelial cells are affected by nicotine in the presence of LSS to truly understand the influence of nicotine in vasculature.

We first evaluated the effect of nicotine associated with different intensities of LSS on HUVECs in respect of morphological alteration. After shearing for 12 h, we found that cells with 10^{-4} M nicotine exhibited higher level of elongation and alignment as compared to the group without nicotine, and such variations augmented along with increase of LSS intensity. We reasoned that this irregular response to LSS occurred

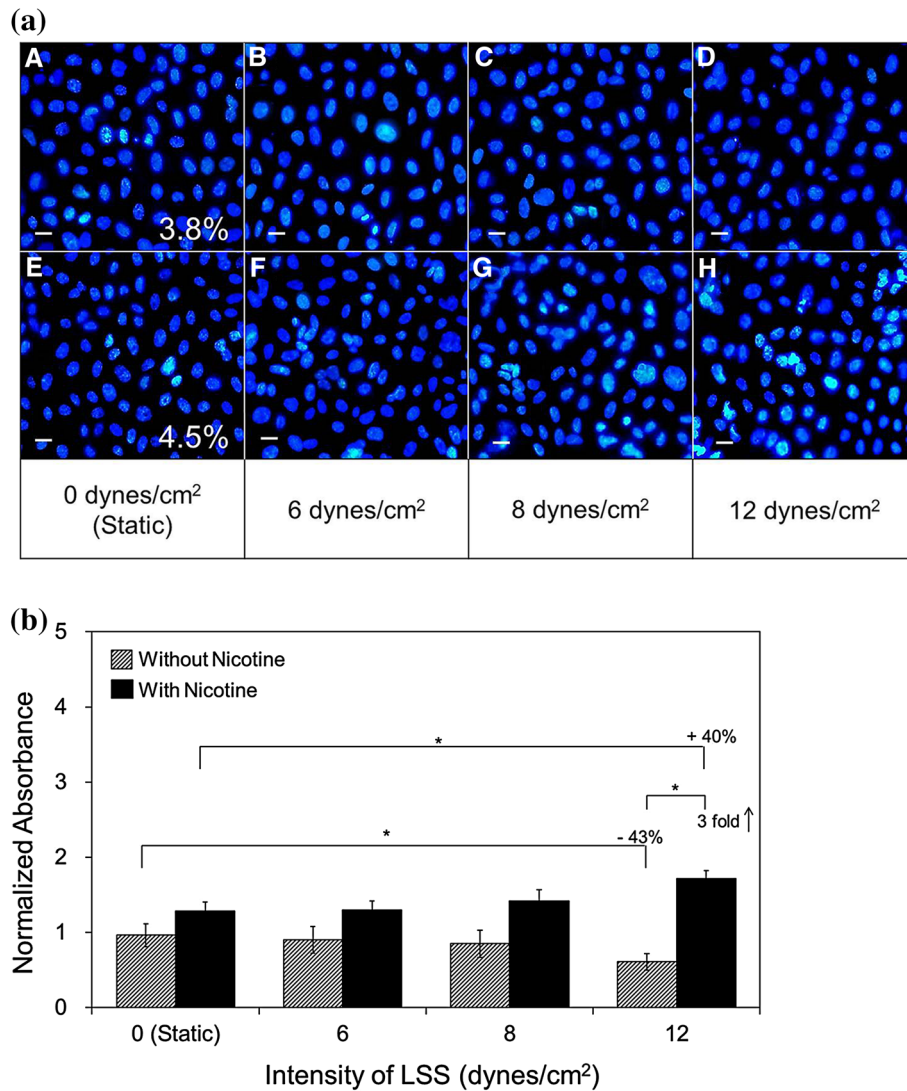


FIGURE 3. Synergistic effect of nicotine and LSS on the endothelial apoptosis. (a) Photomicrographic images of Hoechst 33258 stained HUVEC nuclei sheared by 0 (A and E; static culture), 6 (B and F), 8 (C and G), and 12 (D and H) dynes cm^{-2} LSS using normal (A–D) or nicotine-containing (E–H) medium for 12 h. All images were photographed by an inverted fluorescence microscope at 40 \times magnification. The percentage in image A and E represents the mean ratio of apoptotic cells of the static setting calculated by counting number of apoptotic cells per total cell amount in 60 fluorescent microscopic zones (6 glass slides and 10 microscopic regions for each slide). Scale bar = 15 μm . (b) Quantitative analysis of the HUVECs apoptosis. Both static and sheared HUVECs were treated by media with and without 10^{-4} M nicotine for 12 h, respectively. The apoptotic level of HUVECs in each group was determined by absorbance of cytoplasmic histone-associated DNA fragments detected using an ELISA reader at wavelength of 405 nm. Each absorbance value was presented after normalization to the background signal. Values are mean \pm SE ($n = 3$). * $p < 0.05$.

in the presence of nicotine was likely resulted from the impairment of cellular cytoskeleton due to elevation of reactive oxygen species (ROS) as illustrated in Supplementary Fig. S4 (A, B, D, and E). ROS are O_2 -derived reactive molecules (e.g., superoxide anion, hydroxyl, and hydrogen peroxide) generated from the cellular metabolism. Overproduction of ROS may alter the structure of filament network and lead to endothelial dysfunction accordingly.²⁰ This cytoskeletal impairment can be observed in static cultures with nicotine (Fig. 1b) in which cells shrank and thinned,

and reflected by higher ΔAR and ΔAMAF (Fig. 2) in the sheared cells. In terms of the cells treated with lower concentration (10^{-7} M) of nicotine, it is foreseeable that the efficiency of ROS generation was lower than the group with 10^{-4} M nicotine, resulting in delayed morphological alteration.

We following investigated how the morphological abnormality influences the cell fate *in vitro*. Based on the results of multiple examinations including nuclei staining, DNA fragmentation assay, and detection of PAPR1 expression (Figs. 3, 4), we demonstrated that

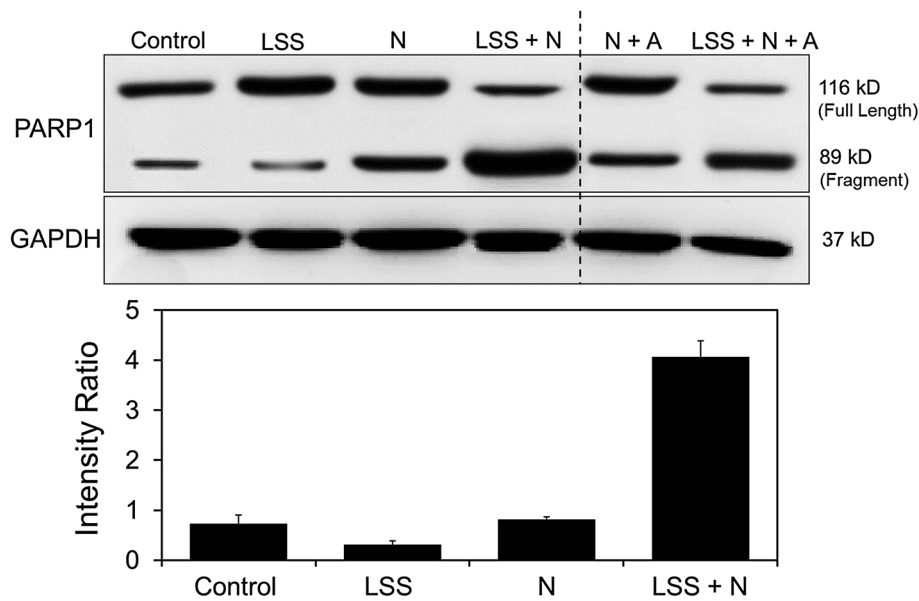


FIGURE 4. Analyses of apoptosis level of HUVECs treated by various conditions. Top: Western blots of PARP1 and GAPDH in HUVECs treated with and without LSS (12 dynes cm^{-2}), nicotine (N; 10^{-4} M), and/or ascorbic acid (A; 10^{-4} M) for 12 h. The condition of each group/lane is indicated on the top of the blotting photograph. Bottom: Quantitative analyses of the western blot data for the groups without ascorbic acid. Apoptosis level of each group was evaluated by the fold change of fragment PARP1 over full length PARP1 which was represented intensity ratio (Intensity ratio = optical density level of cleaved PARP1/optical density level of full length PARP1). The optical density level of each PARP1 blot was normalized to GAPDH prior to calculation. Values are mean \pm SE ($n = 3$). The western blot data of the group treated with LSS, nicotine, and ascorbic acid (LSS + N + A) was quantitatively analyzed and presented in Fig. 8, whereas the group treated with nicotine and ascorbic acid in static (N + A) was provided as a reference in this study.

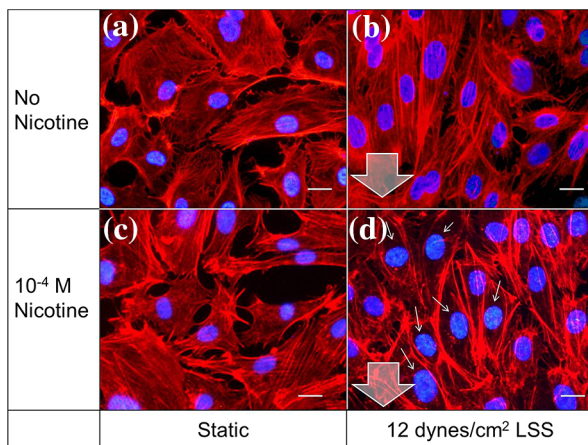


FIGURE 5. Photomicrographic images of HUVECs stained for stress fibers (red) and nuclei (blue). (a) Static cultures without nicotine (control). (b) Cells sheared by 12 dynes cm^{-2} LSS using normal medium for 12 h. Note abundance of actin cytoskeletons near the nuclei. (c) Static cultures with 10^{-4} M nicotine exposure for 12 h. (d) Cells sheared by 12 dynes cm^{-2} LSS using 10^{-4} M nicotine medium for 12 h. Note rearrangement of fibers with depletion of actin cytoskeletons near the nuclei. All images were photographed using an inverted fluorescence microscope at $40\times$ magnification. Big arrows denote the flow direction. Small arrows indicate the cytoskeletal disaggregation near the nucleus. Scale bar = $15 \mu\text{m}$.

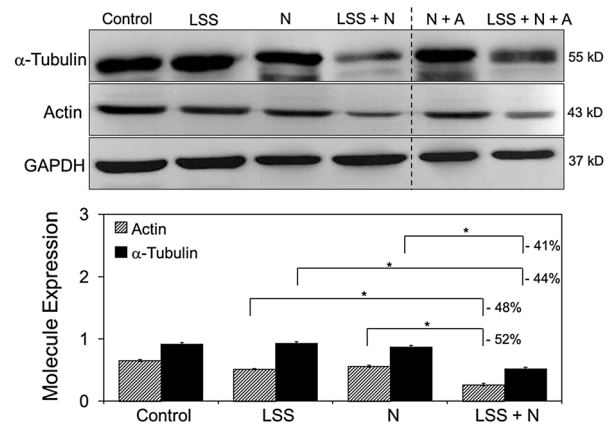


FIGURE 6. Analyses of cytoskeletal expressions of HUVECs treated by various conditions. Top: Western blots of α -tubulin, actin and GAPDH in HUVECs treated with and without LSS (12 dynes cm^{-2}), nicotine (N; 10^{-4} M), and/or ascorbic acid (A; 10^{-4} M) for 12 h. The condition of each group/lane is indicated on the top of the blotting photograph. Bottom: Quantitative analyses of α -tubulin and total actin expressions for the groups without ascorbic acid. Each bar represents relative optical density level of the molecule as compared to GAPDH. Values are mean \pm SE ($n = 3$). * $p < 0.05$. The western blot data of the group treated with LSS, nicotine, and ascorbic acid (LSS + N + A) was quantitatively analyzed and presented in Fig. 7b, whereas the group treated with nicotine and ascorbic acid in static (N + A) was provided as a reference in this study.

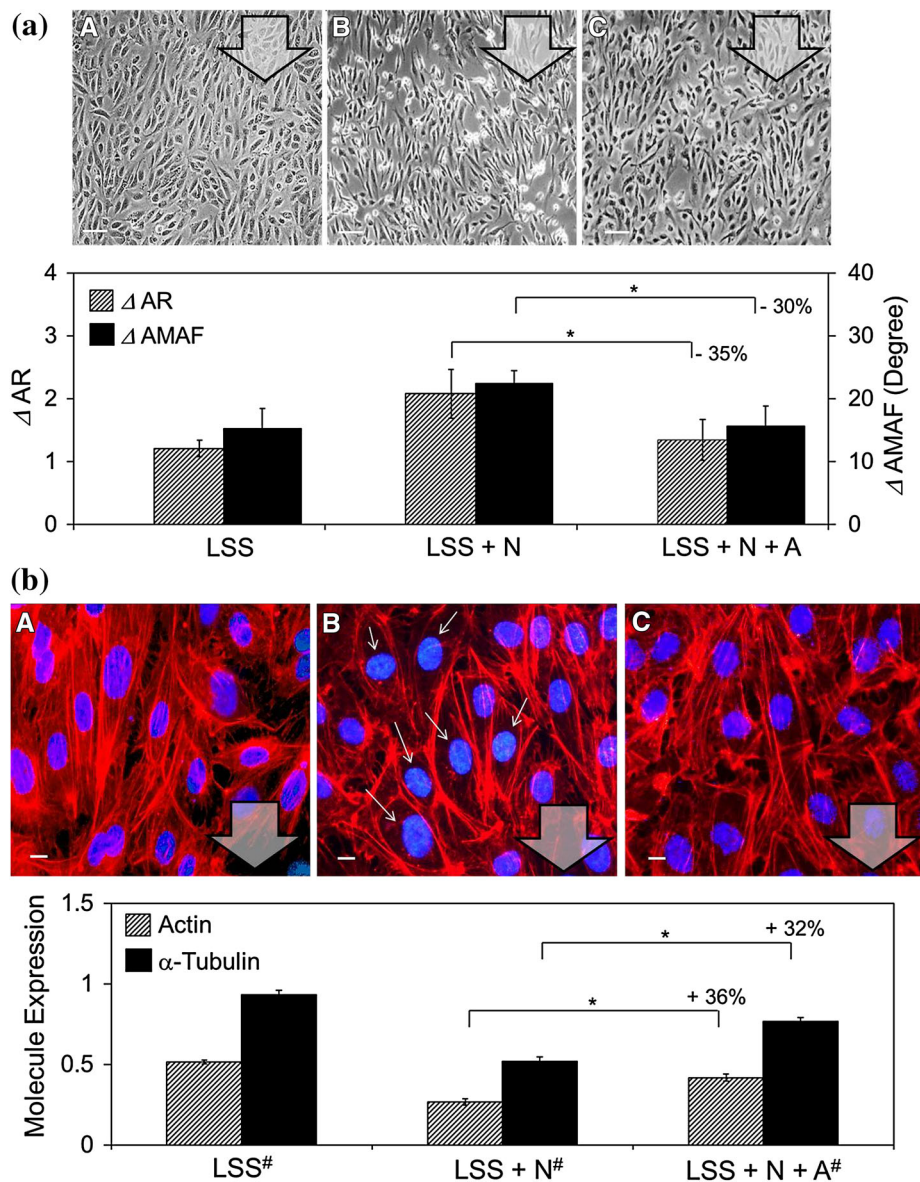


FIGURE 7. Efficacy of ascorbic acid to reduce HUVECs impairments resulted from synergistic effect of nicotine and LSS. (a) Analyses of cellular morphological reorganization. The upper photomicrographs represent phase contrast images of HUVECs sheared by 12 dynes cm^{-2} LSS using A: normal growth medium (LSS); B: nicotine-containing medium (LSS + N; 10^{-4} M); and C: nicotine and ascorbic acid-containing medium (LSS + N + A; 10^{-4} M for each chemical). Images were photographed at $20\times$ magnification. Arrows indicate the flow direction. Scale bar = $100 \mu\text{m}$. The bottom bar chart represents the quantitative analyses of cellular morphological reorganization through calculations of ΔAR and $\Delta AMAF$. Values are mean \pm SE ($n = 3$). $*p < 0.05$. (b) Analyses of α -tubulin and total actin expressions. The upper photomicrographs represent rhodamine phalloidin-stained stress fibers and Hoechst 33258-stained nuclei for HUVECs sheared by 12 dynes cm^{-2} LSS using A: normal growth medium (LSS); B: nicotine-containing medium (LSS + N; 10^{-4} M); and C: nicotine and ascorbic acid-containing medium (LSS + N + A; 10^{-4} M for each chemical). Images were photographed at $40\times$ magnification. Big arrows denote the flow direction. Small arrows indicate the cytoskeletal disaggregation near the nucleus. Scale bar = $15 \mu\text{m}$. The bottom bar chart represents the relative optical density level of each protein molecule as compared to GAPDH. Values are mean \pm SE ($n = 3$). #Denotes the western blot results shown in Fig. 6. $*p < 0.05$.

10^{-4} M nicotine with 12-h exposure has no distinguishable effect on endothelial apoptosis that is similar with previous study.³² In addition, inhibitory effect of apoptosis indeed appeared in the LSS-treated HUVECs since LSS-induced reorganization enabled to minimize the total forces on the cellular luminal

surfaces and facilitate formation and/or expression of cytoskeletons, offering protective effect to endothelial cells including anti-apoptosis.³¹ However, the cellular apoptosis dramatically increased while they were treated with nicotine and LSS simultaneously, and the level of induced apoptosis was positively related to the

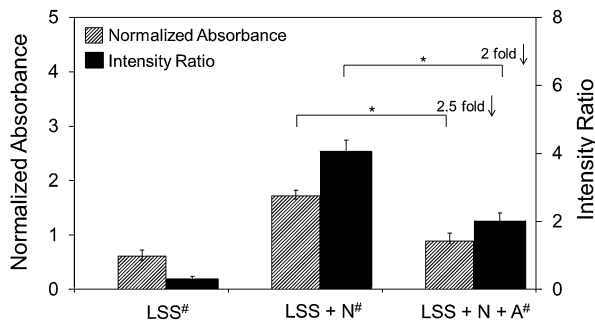


FIGURE 8. Efficacy of ascorbic acid on reduction of the HUVECs apoptosis caused by synergistic impact of nicotine and LSS. All samples were sheared by 12 dynes cm^{-2} LSS for 12 h using normal growth medium (LSS), nicotine-containing medium (LSS + N; 10^{-4} M), and nicotine and ascorbic acid-containing medium (LSS + N + A; 10^{-4} M for each chemical). The apoptotic level of each group was determined by the absorbance of cytoplasmic histone-associated DNA fragments normalized to the background signal (left Y-axis) and intensity ratio of fragment to full length of PARP1 molecules expression (right Y-axis). Values are mean \pm SE ($n = 3$). #Denotes the western blot results shown in Fig. 4. * $p < 0.05$.

intensity of LSS used. These findings suggest a strong correlation between cell apoptosis and excessive morphological change, and indicate that LSS does play an adverse role in nicotine-associated vascular injury. These results support the clinical consequence that nicotine (or cigarette smoking) is highly associated with proximal vessel disease in which high shear stress plays a key role in the lesion.

The type and molecular basis of aforementioned cell death can be further clarified through the examination of PARP1 expression. PARP1 is a nuclear enzyme that can be specifically proteolysed by caspases to form catalytic fragments,¹⁶ and this cleavage enables to promote apoptosis by preventing DNA repair-induced survival and by blocking energy depletion-induced necrosis.⁸ Therefore, the increase of PARP1 fragment is a decisive evidence of cellular apoptosis. Based on the fact that expression of cleaved PARP1 enhanced in the group with dual stimulations (Fig. 4; LSS + N), it is assured that the aforementioned cell death was apoptosis instead of necrosis, and was processed through poly(ADP-ribosylation).⁸ However, more studies are certainly needed to fully address the detailed molecular pathway of the induced apoptosis.

How would the apoptosis occur and associate with excessive morphological change? We surmised that the apoptosis was resulted from the interruption of mechanostasis due to cytoskeletal disruption caused from irregular morphological reorganization. Mechanical homeostasis, herein termed mechanostasis, means the tendency of cells and/or tissues to maintain equilibrium of physiological mechanical loadings. Cellular mechanostasis is highly regulated by mechanical signals transduced between cellular

contacts, adhesion receptors and intracellular cytoskeletons (i.e., mechanotransduction).⁶ Disruption of cellular cytoskeleton will interrupt mechanotransduction and trigger apoptotic response as reported previously.⁵ This hypothesis was confirmed by collapsed actin cytoskeleton (Fig. 5d) and reduced expressions of actin and α -tubulin in the group with dual stimulations (Fig. 6; LSS + N). Furthermore, our data showed that the apoptotic level of the cells which were sheared with nicotine-containing medium (10^{-4} M) was positively related to the degree of cytoskeletal disaggregation within 12 h of treatment (Supplementary Fig. S5; D/d and E/e), indicating the cell apoptosis is highly correlated with cytoskeletal injury.

Finally we sought to verify the role of oxidative stress in cytoskeletal disintegration and consequent apoptosis by adding ascorbic acid, a commonly used free radical scavenger in the flushing medium. Ascorbic acid is a water-soluble vitamin (Vitamin C) and its diverse biological functions have been extensively identified in the past decades since it was first isolated in 1928. In addition to serving as an antioxidant, ascorbic acid is essential for the development and maintenance of human connective tissues (e.g., bone formation, wound healing and gum maintenance), and plays an important role in a number of metabolic functions including the activation of the B vitamin and folic acid; the conversion of cholesterol, amino acid, tryptophan to bile acids, neurotransmitter, and serotonin, respectively. Moreover, it has also been widely used as a supplementary agent for disease prevention, enhancement of immune system, and/or reduction of allergic reactions.¹⁵ In this study, the function of anti-oxidation of ascorbic acid was exploited and the competency of 10^{-4} M ascorbic acid on reduction of intracellular ROS level was preliminarily verified as shown in Supplementary Fig. S4. Our results showed that the irregular morphological alteration (Fig. 7a), decomplexification of cytoskeleton (Fig. 7b) and elevated apoptosis (Figs. 4, 8) were all significantly arrested by use of ascorbic acid, manifesting that oxidative stress certainly played a detrimental role in endothelial damage caused by synergistic impact of nicotine and LSS. In addition, it has been reported that endothelial cells exposed to cyclic strain have increased ROS production^{7,22} as compared to the group cultivated statically, and arterial endothelium *in vivo* is exposed to higher cyclic strain than is venous endothelium.³ Therefore, it is foreseeable that ROS production in arteries can be elevated by cyclic strain and such facilitation of oxidative stress may further enhance the cellular apoptosis led by synergistic impact of nicotine and LSS *in vivo* and complicate the nicotine-mediated vascular lesions accordingly. Overall, the efforts presented in this study have prompted a clinical

interest since therapy against free radicals may be helpful to mitigate nicotine-associated vascular injury.

In summary, we have demonstrated, for the first time, that synergistic impact of nicotine and LSS with strength of ≥ 12 dynes cm^{-2} may cause cytoskeleton disintegration and enhanced apoptosis for endothelial cells. All the experiments were conducted in the parallel plate flow system that brought this study closer to the physiological condition (i.e., hemodynamic environment). Since endothelial apoptosis enables to accelerate many cardiovascular diseases through a series of lesions,²⁷ the efforts presented in this study may provide an explanation for the strong correlation between proximal vessel disease and smoking. However, considering the nicotine concentration used in this study is higher than the mean plasma nicotine concentration found in most of cigarette smokers (10^{-6} – 10^{-7} M),¹⁴ further investigations using nicotine at physiological level with wider range of LSS magnitudes and/or prolonged shearing time will be performed to fully address the detrimental effects found and efforts are currently in progress.

ELECTRONIC SUPPLEMENTARY MATERIAL

The online version of this article (doi: [10.1007/s10439-014-1244-9](https://doi.org/10.1007/s10439-014-1244-9)) contains supplementary material, which is available to authorized users.

ACKNOWLEDGMENTS

This work was financially supported by National Science Council of Taiwan, R.O.C. NSC 101-2221-E-008-018 (Y.-H. Lee).

CONFLICT OF INTEREST

None of the author in this paper has declared any conflict of interest.

REFERENCES

- ¹Aboyans, V., P. Lacroix, and M. H. Criqui. Large and small vessels atherosclerosis: similarities and differences. *Prog. Cardiovasc. Dis.* 50:112–125, 2007.
- ²Ando, J., and K. Yamamoto. Vascular mechanobiology: endothelial cell responses to fluid shear stress. *Circ. J. / Emphasis > 73:1983–1992*, 2009.
- ³Bundey, R. A. Endothelial cell mechanosensitivity. Focus on “Cyclic strain and motion control produce opposite oxidative responses in two human endothelial cell types”. *Am. J. Physiol. Cell Physiol.* 293:C33–C34, 2007.
- ⁴Cardinale, A., C. Nastrucci, A. Cesario, and P. Russo. Nicotine: specific role in angiogenesis, proliferation and apoptosis. *Crit. Rev. Toxicol.* 42:68–89, 2012.
- ⁵Chan, D. D., W. S. Van Dyke, M. Bahls, S. D. Connell, P. Critser, J. E. Kelleher, M. A. Kramer, S. M. Pearce, S. Sharma, and C. P. Neu. Mechanostasis in apoptosis and medicine. *Prog. Biophys. Mol. Biol.* 106:517–524, 2011.
- ⁶Chen, C. S., J. Tan, and J. Tien. Mechanotransduction at cell-matrix and cell-cell contacts. *Annu. Rev. Biomed. Eng.* 6:275–302, 2004.
- ⁷Cheng, J. J., B. S. Wung, Y. J. Chao, H. J. Hsieh, and D. L. Wang. Cyclic strain induces redox changes in endothelial cells. *Chin. J. Physiol.* 42:103–111, 1999.
- ⁸D’Amours, D., F. R. Sallmann, V. M. Dixit, and G. G. Poirier. Gain-of-function of poly(ADP-ribose) polymerase-1 upon cleavage by apoptotic proteases: implications for apoptosis. *J. Cell. Sci.* 114:3771–3778, 2001.
- ⁹Diehm, N., A. Shang, A. Silvestro, D. D. Do, F. Dick, J. Schmidli, F. Mahler, and I. Baumgartner. Association of cardiovascular risk factors with pattern of lower limb atherosclerosis in 2659 patients undergoing angioplasty. *Eur. J. Vasc. Endovasc. Surg.* 31:59–63, 2006.
- ¹⁰Dimmeler, S., C. Hermann, J. Galle, and A. M. Zeiher. Upregulation of superoxide dismutase and nitric oxide synthase mediates the apoptosis-suppressive effects of shear stress on endothelial cells. *Arterioscler. Thromb. Vasc. Biol.* 19:656–664, 1999.
- ¹¹Duchene, J., C. Cayla, S. Vessillier, R. Scotland, K. Yamashiro, F. Lecomte, I. Syed, P. Vo, A. Marrelli, C. Pitzalis, F. Cipollone, J. Schanstra, J. L. Bascands, A. J. Hobbs, M. Perretti, and A. Ahluwalia. Laminar shear stress regulates endothelial kinin B1 receptor expression and function: potential implication in atherogenesis. *Arterioscler. Thromb. Vasc. Biol.* 29:1757–1763, 2009.
- ¹²Fitzpatrick, P. A., A. F. Guinan, T. G. Walsh, R. P. Murphy, M. T. Killeen, N. P. Tobin, A. R. Pierotti, and P. M. Cummins. Down-regulation of neprilysin (EC3.4.24.11) expression in vascular endothelial cells by laminar shear stress involves NADPH oxidase-dependent ROS production. *Int. J. Biochem. Cell Biol.* 41:2287–2294, 2009.
- ¹³Haltmayer, M., T. Mueller, W. Horvath, C. Luft, W. Poelz, and D. Haidinger. Impact of atherosclerotic risk factors on the anatomical distribution of peripheral arterial disease. *Int. Angiol.* 20:200–207, 2001.
- ¹⁴Hukkanen, J., P. Jacob, and N. L. Benowitz. Metabolism and disposition kinetics of nicotine. *Pharmacol. Rev.* 57:79–115, 2005.
- ¹⁵Iqbal, K., A. Khan, and M. M. A. K. Khattak. Biological significance of ascorbic acid (vitamin C) in human health—a review. *Pak. J. Nutr.* 3:5–13, 2004.
- ¹⁶Kaufmann, S. H., S. Desnoyers, Y. Ottaviano, N. E. Davidson, and G. G. Poirier. Specific proteolytic cleavage of poly(ADP-ribose) polymerase: an early marker of chemotherapy-induced apoptosis. *Cancer Res.* 53:3976–3985, 1993.
- ¹⁷Lee, J., and J. P. Cooke. The role of nicotine in the pathogenesis of atherosclerosis. *Atherosclerosis* 215:281–283, 2011.
- ¹⁸Levesque, M. J., and R. M. Nerem. The elongation and orientation of cultured endothelial cells in response to shear stress. *J. Biomech. Eng.* 107:341–347, 1985.
- ¹⁹Ling, Y., N. Lu, Y. Gao, Y. Chen, S. Wang, Y. Yang, and Q. Guo. Endostar induces apoptotic effects in HUVECs

- through activation of caspase-3 and decrease of Bcl-2. *Anticancer Res.* 29:411–417, 2009.
- ²⁰Lum, H., and K. A. Roebuck. Oxidant stress and endothelial cell dysfunction. *Am. J. Physiol. Cell. Physiol.* 280:C719–C741, 2001.
- ²¹Malek, A. M., S. L. Alper, and S. Izumo. Hemodynamic shear stress and its role in atherosclerosis. *JAMA. J. Am. Med. Assoc.* 282:2035–2042, 1999.
- ²²Matsushita, H., K. H. Lee, and P. S. Tsao. Cyclic strain induces reactive oxygen species production via an endothelial NAD(P)H oxidase. *J. Cell Biochem. Suppl. Suppl* 36:99–106, 2001.
- ²³Ray, S., O. Bucur, and A. Almasan. Sensitization of prostate carcinoma cells to Apo2L/TRAIL by a Bcl-2 family protein inhibitor. *Apoptosis* 10:1411–1418, 2005.
- ²⁴Rennier, K., and J. Y. Ji. Shear stress regulates expression of death-associated protein kinase in suppressing TNF α -induced endothelial apoptosis. *J. Cell. Physiol.* 227:2398–2411, 2012.
- ²⁵Sackett, D. L., R. W. Gibson, I. D. Bross, and J. W. Pickren. Relation between aortic atherosclerosis and the use of cigarettes and alcohol. An autopsy study. *N. Engl. J. Med.* 279:1413–1420, 1968.
- ²⁶Smith, F. B., A. J. Lee, F. G. Fowkes, A. Rumley, and G. D. Lowe. Smoking, haemostatic factors and the severity of aorto-iliac and femoro-popliteal disease. *Thromb. Haemost.* 75:19–24, 1996.
- ²⁷Stoneman, V. E., and M. R. Bennett. Role of apoptosis in atherosclerosis and its therapeutic implications. *Clin. Sci. (Lond)* 107:343–354, 2004.
- ²⁸Takabe, W., E. Warabi, and N. Noguchi. Anti-atherogenic effect of laminar shear stress via Nrf2 activation. *Antioxid. Redox. Signal.* 15:1415–1426, 2011.
- ²⁹Traub, O., and B. Berk. Laminar shear stress: mechanisms by which endothelial cells transduce an atheroprotective force. *Arterioscler. Thromb.* 18:677–685, 1998.
- ³⁰Wang, W., C. H. Ha, B. S. Jhun, C. Wong, M. K. Jain, and Z. G. Jin. Fluid shear stress stimulates phosphorylation-dependent nuclear export of HDAC5 and mediates expression of KLF2 and eNOS. *Blood* 115:2971–2979, 2010.
- ³¹Wu, C. C., Y. S. Li, J. H. Haga, R. Kaunas, J. J. Chiu, F. C. Su, S. Usami, and S. Chien. Directional shear flow and Rho activation prevent the endothelial cell apoptosis induced by micropatterned anisotropic geometry. *Proc. Natl. Acad. Sci. USA* 104:1254–1259, 2007.
- ³²Yang, Y. M., and G. T. Liu. Damaging effect of cigarette smoke extract on primary cultured human umbilical vein endothelial cells and its mechanism. *Biomed. Environ. Sci.* 17:121–134, 2004.
- ³³Yegutkin, G., P. Bodin, and G. Burnstock. Effect of shear stress on the release of soluble ecto-enzymes ATPase and 5'-nucleotidase along with endogenous ATP from vascular endothelial cells. *Br. J. Pharmacol.* 129:921–926, 2000.
- ³⁴Zarins, C. K., M. A. Zatina, D. P. Giddens, D. N. Ku, and S. Glagov. Shear stress regulation of artery lumen diameter in experimental atherogenesis. *J. Vasc. Surg.* 5:413–420, 1987.
- ³⁵Zeidler, R., K. Albermann, and S. Lang. Nicotine and apoptosis. *Apoptosis* 12:1927–1943, 2007.